Accepted Manuscript

Accurate determination of key surface properties that determine the efficient separation of bovine milk BSA and LF proteins

Virginia Valiño, Ma Fresnedo San Román, Raquel Ibá ñez, José M. Benito, Isabel Escudero, Inmaculada Ortiz

Please cite this article as: V. Valiño, M.F.S. Román, R. Ibá ñez, J.M. Benito, I. Escudero, I. Ortiz, Accurate determination of key surface properties that determine the efficient separation of bovine milk BSA and LF proteins, *Separation and Purification Technology* (2014), doi: http://dx.doi.org/10.1016/j.seppur.2014.07.051

This is a PDF file of an unedited manuscript that has been accepted for publication. As a service to our customers we are providing this early version of the manuscript. The manuscript will undergo copyediting, typesetting, and review of the resulting proof before it is published in its final form. Please note that during the production process errors may be discovered which could affect the content, and all legal disclaimers that apply to the journal pertain.

Accurate determination of key surface properties that determine the efficient separation of bovine milk BSA and LF proteins.

Virginia Valiño[a], Ma Fresnedo San Román[a], Raquel Ibáñez[a], José M. Benito[b], Isabel Escudero[b], Inmaculada Ortiz[a]*

[a]Departamento de Ingenierías Química y Biomolecular, ETSIIyT, Universidad de Cantabria

Avda. los Castros s/n, 39005 Santander, Spain

[b]Departamento de Biotecnología y Ciencia de los Alimentos, Facultad de Ciencias, Universidad de Burgos

Plaza Misael Bañuelos s/n, 09001 Burgos, Spain

*Email: inmaculada.ortiz@unican.es   Phone: +34 942 201585, Fax: +34 942 201591

Abstract

The aim of this work is to accurately measure fundamental surface properties, i.e., zeta potential, isoelectric point and protein size that determine the optimal separation conditions of Bovine serum albumin and lactoferrin, two high added value food proteins whose similarity in weight makes their separation a scientific and technical challenge.

The systematic study of these proteins' surface properties was performed under different conditions: i) 3.0 < pH < 10.0, ii) electrolyte type: KCl, NaCl and $CaCl_2$ and concentration (0.01 - 0.1 M KCl) and iii) protein concentration in the range of 0.04 – 4.0 g L^{-1} for BSA and 0.01 – 1.0 g L^{-1} for LF with the objective of establishing the optimal separation conditions.

Finally, the comparison of the experimental and theoretically calculated values revealed significant deviations under specific conditions, highlighting the simplicity of the theoretical assumptions and leading to the conclusion that the use of experimental surface properties is still needed for the correct design of food protein separation processes.

List of symbols

C	concentration (mol m^{-3})
d	particle size (nm)
e	electron charge (1.602×10^{-19} C)
F	Faraday's constant (96484.56 C mol^{-1})
ƒ(κa)	Henry's function

f/f_0	frictional ratio
f	frictional coefficient
f_0	theoretical frictional coefficient
I	ionic strength (mol L^{-1})
Ip	isoelectric point
k	Boltzmann constant (1.38×10^{-23} J K^{-1})
K^{int}	intrinsic equilibrium constants
K_j	equilibrium constant of Cl$^-$ binding sites
L_D	Debye length (nm)
m_j	number of Cl$^-$ binding sites
M_W	molecular weight (kDa)
N	Avogadro's number (6.022×10^{23} mol^{-1})
n_i	number of titratable amino acids
P	pressure (Pa)
PdI	polydispersity index
R	gas constant (8.314 J mol^{-1} K^{-1})
r_S	Solute radius (nm)
r	Stokes radius (nm)
T	absolute temperature (K)
v	partial specific volume (m^3 g^{-1})
z	protein surface charge (mV)
z_i	ion valence
Z_{ion}^-	anions charge contribution (mV)
Z_H^+	cations charge contribution (mV)
z_{max}	total number of positively charged amino acid residues at very low pH
$Z_{protein}$	protein net charge (mV)

Greek letters

ε_i	dielectric constant of the fluid (78.5)
ε_o	electrical permittivity of vacuum (8.854×10^{-12} C V^{-1} m^{-1})
κ^{-1}	thickness of the electrical double layer (m)
μ_E	electrophoretic mobility (cm s^{-1} V^{-1})
ψ_s^*	electrostatic potential at the protein surface (V)
σ_S^*	effective surface density (C m^{-2})
γ	activity coefficient of the ion

η sample dynamic viscosity (N s m^{-2})

ζ zeta potential (mV)

1. Introduction

Bovine whey proteins have been increasingly used as food ingredients, mainly due to their well-balanced amino acid formulation and their functional properties, including the ability to form gels, their solubility and their foaming and emulsifying characteristics [1]. Whey is a high and varied mixture of secreted proteins, which contain a wide range of chemical, physical, and functional properties [2]. Among them, bovine serum albumin (BSA) has foaming and gelling properties and bovine lactoferrin (LF) presents important nutraceutical and anti-inflammatory or antimicrobial properties and plays a significant role in iron metabolism [3]. Such properties made its use interesting in food and pharmaceutical applications. The separation of proteins from their original mixtures is usually carried out through costly downstream processes that can account for as much as 80 % of the entire production cost [4]. Cheng et al., 2008 [5] reported that there are many challenges that make protein separation a difficult task, thus it seems to be infeasible to develop an all-embracing principle for protein separation based solely on single protein characteristics.

It is well established that protein transport through semipermeable ultrafiltration membranes, (widely used for protein separation in food processing [6]) can be strongly affected by electrostatic interactions between the charged membrane and the charged protein. Furthermore, due to the nature of protein interactions, protein aggregation may occur, leading to differences in size, shape and morphology. The understanding of the interactions, causes and analyses of such aggregates is a key factor to control protein aggregation permitting successful separations [7].

To maximize the effectiveness of the separation processes, an accurate description of the effect of physicochemical interactions between protein molecules is necessary [8]. Particle size measurements allow the correct selection of the membrane cut-off, as well as the proper prediction of protein aggregation and foaming, thus allowing for the correct selection of buffers, pH and temperatures for storage [7]. The description of the protein surface properties can be performed by zeta potential and particle size measurements through electrophoretic light scattering (ELS) and dynamic light scattering (DLS) techniques, respectively. Such measurements may be made in free solution and over a wide range of ionic strength and pH [9].

Even though multiple articles on the analysis of protein properties have been published [10–17], there is a gap concerning the determination of the properties of proteins with similar characteristics found in the same natural media, such as bovine serum albumin (BSA) and bovine lactoferrin (LF).

This work investigated the principal surface properties such as zeta potential, isoelectric point and protein size of two minor milk whey proteins in different conditions of electrolyte type and concentration, protein concentration and pH. Bovine serum albumin (BSA) is a 65.0 kDa protein with a theoretical isoelectric point (Ip) of approximately 5.0. The BSA concentration in milk whey is on average 0.4 g L^{-1} [18]. Bovine lactoferrin (LF) is a 78.0 kDa iron-binding protein with a theoretical Ip between 7.0 and 9.0. LF is present at an average concentration of 0.1 g L^{-1} in milk whey [19]. Because of the similarity in the properties of the two proteins, their correct quantification would be of great value in the establishment of operational conditions leading to maximum flux and selectivity for separation and purification processes of BSA/LF protein by ultrafiltration technology with charged membranes. These conditions are related to the maximum difference between protein zeta potential and protein size.

2. Materials and methods

4

2.1. Protein solutions

Experiments were performed using native bovine serum albumin with a purity higher than 96.0 % (Catalogue A-6003 Sigma Chemical, Madrid, Spain) and native lactoferrin purified to 98.0 % with a Fe^{3+} content of 3.0 mg/100.0 g of protein (NutriScience Innovations, LLC Trumbull, CT USA). The electrolytes used were prepared by dissolving the corresponding amount of KCl, NaCl and $CaCl_2$ (analytical grade, Panreac, Spain). The pH was adjusted by adding 0.1 M HCl and NaOH (TitriPUR®, Merck Millipore). The BSA/LF concentration ratio always kept the value 4.0/1.0, characteristic of milk whey. The solutions were prepared avoiding dispersion. All the samples were clear and transparent.

2.2. Light scattering analysis

Protein physicochemical properties were characterized with a Zetasizer Nano ZS (Malvern Instruments, United Kingdom). The charge of the proteins as a function of pH, electrolyte type, ionic strength and protein concentration was determined by phase analysis light scattering (PALS) using the Henry equation and applying the Hückel approximation (Appendix A). The net protein charge was obtained using an adapted form of the charge regulation model originally developed by Tanford et al.,1955 [20] and Scatchard et al., 1959 [21] (Appendix B), as a function of the solution environment (pH and ionic strength), which allowed the determination of the theoretical isoelectric points (Ip) and comparison to the experimental values.

The size and aggregation were evaluated by dynamic light scattering (DLS) by the diffusion coefficient (D_{app}) using the Stokes-Einstein equation (More information can be found in Appendix A). The hydrodynamic radius, or Stokes radius, which considers the protein as a hard sphere with laminar movement in a continuous solvent [22], was determined to compare the results with the experimental data (Appendix B).

3. Results and discussion

3.1. Zeta potential measurements

Protein charge plays an important role in the performance of separation processes, being of special relevance when charged membranes are involved. In this work the zeta potential of BSA and LF solutions was measured under different operational conditions relevant to the separation process.

Influence of the electrolyte type and concentration on the zeta potential and Ip of bovine milk proteins

First, the influence of the electrolyte type, using 0.01 M solutions of KCl, NaCl and $CaCl_2$, on the zeta potential of 4.0 g L^{-1} of BSA and 1.0 g L^{-1} of LF solutions was determined. Figure 1 plots the change in the zeta potential for both proteins with pH; experimental data are plotted together with error bars obtained from replication of the measurements and show that the relative error is less than 13% in all cases. The Ip of both proteins falls inside the studied pH range. When the pH is lower than the Ip, the biomolecules present positive zeta potential values that decrease with increasing pH.
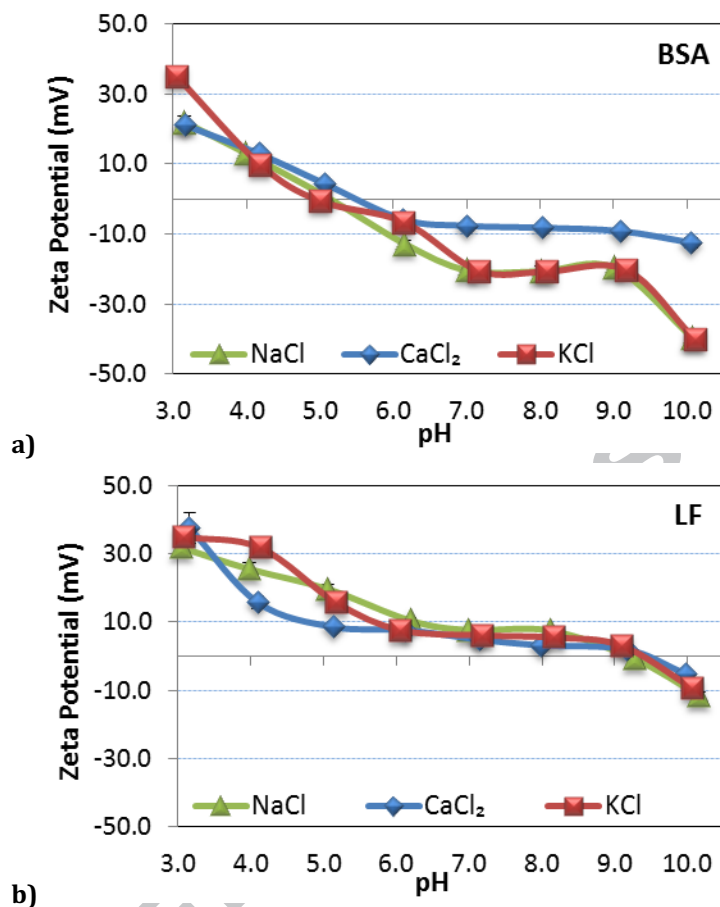
Figure 1. Change in zeta potential with pH for different electrolytes: a) BSA and b) LF.

With regard to the influence of the electrolyte type, Figure 1a confirms that the difference in the zeta potential values of BSA when using different electrolytes (1:1 and 1:2) appeared to be significant above the isoelectric point, whereas in the case of LF this difference appears below the isoelectric point (Figure 1b). This behavior can be theoretically described by the dependency of the zeta potential on the ionic strength that results by combining equations A1 and B5 (Appendix A and B). Thus, it is expected that 1:2 type electrolytes, which exert a greater contribution to the ionic strength for the same concentration level than 1:1 type electrolytes, will have lower zeta potential values than the latter due to the compression of the electrical double layer thickness. The calculated values of this Debye layer (equation 5B Appendix B) are 96.2 nm for KCl and NaCl and 60.8 nm for $CaCl_2$.

7

Zeta potential of -20.0 mV for BSA and 7.7 mV for LF were obtained working with KCl and NaCl electrolytes at pH 7.0 being the difference of these values the highest observed. Under the selected conditions the separation BSA/LF by ultrafiltration using charged membranes is expected to be enhanced.

Influence of the ionic strength

Food proteins can be present in different mediums that contain different salt concentration or ionic strength, variables that may influence their behavior. The analysis of the influence of the ionic strength on 4.0 g L^{-1} of BSA and 1.0 g L^{-1} of LF was carried out using KCl solutions in the concentration range of 0.01-0.1 M and the pH range of 3.0-10.0. Figure 2 shows the change in zeta potential for both proteins under the studied conditions.
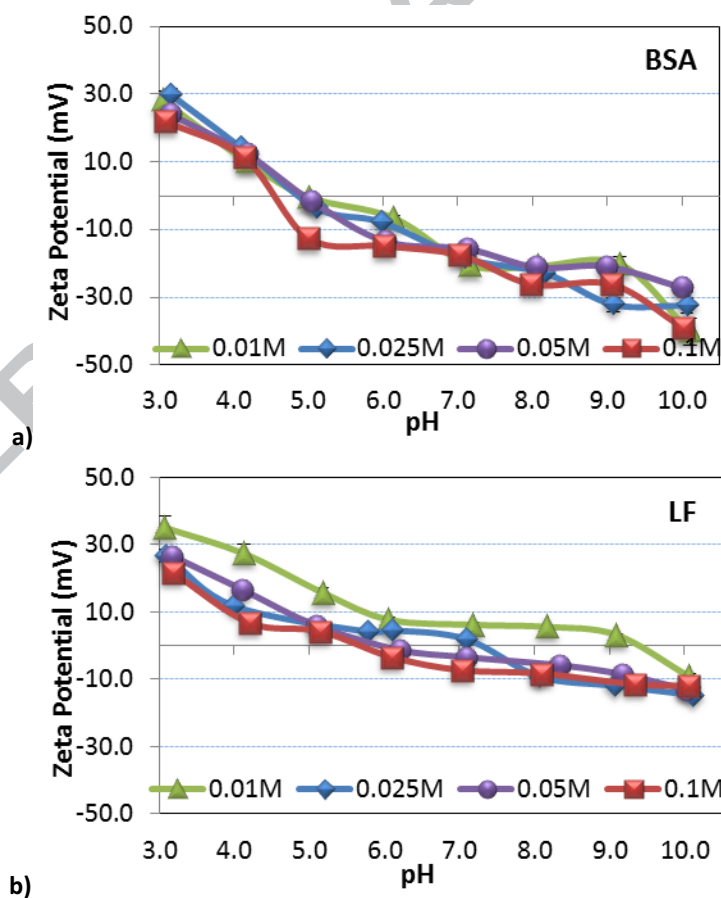

Figure 2. Change in zeta potential with pH for different ionic strengths: a) BSA and b) LF.

As it is shown in Figure 2, both proteins behaved in a similar way. The zeta potential values varied from 30.0 mV to -40.0 mV for BSA and from 35.0 mV to -15.0 mV for LF. The isoelectric point of BSA was the same for the 0.01-0.05 M KCl solutions (4.9-4.96) and was slightly lower value for the highest studied concentration of 0.1 M (4.65). Similar trends have been reported previously [23].

In the case of LF, the effect of the electrolyte concentration on the zeta potential was more significant, with values isoelectric point ranging from 9.3 (0.01 M) to 5.7 (0.1 M). This is consistent with the large range of isoelectric points that have been reported so far for this protein (8.0 – 9.0 for 0.01 M NaCl [24]; 7.2 for 0.025 M KCl [25]; 5.6 for 0.15 M NaCl [12]). It is well known that when the electrolyte concentration is increased, the surface charge is compensated at a lower distance from the particle surface and thus, the surface potential drops faster and the diffuse layer is thinner. Consequently, the measured zeta potential should decrease with increasing electrolyte concentration [11].

When KCl is used as electrolyte the highest difference between zeta potential of both proteins is obtained at pH 7.0 with concentrations 0.01 M and 0.025 M. The zeta potential values were around -19.0mV for BSA and 7.0 mV for LF.

Influence of protein concentration

Any separation/purification process results in a change in the protein concentration. Therefore, the influence of this variable on the zeta potential in the range of 0.04–4.0 g L^{-1} for BSA and 0.01–1.0 g L^{-1} for LF was analyzed. Figure 3 depicts the change in zeta potential for BSA, LF and their mixture as a function of pH for different protein concentrations using 0.025 M KCl.

9
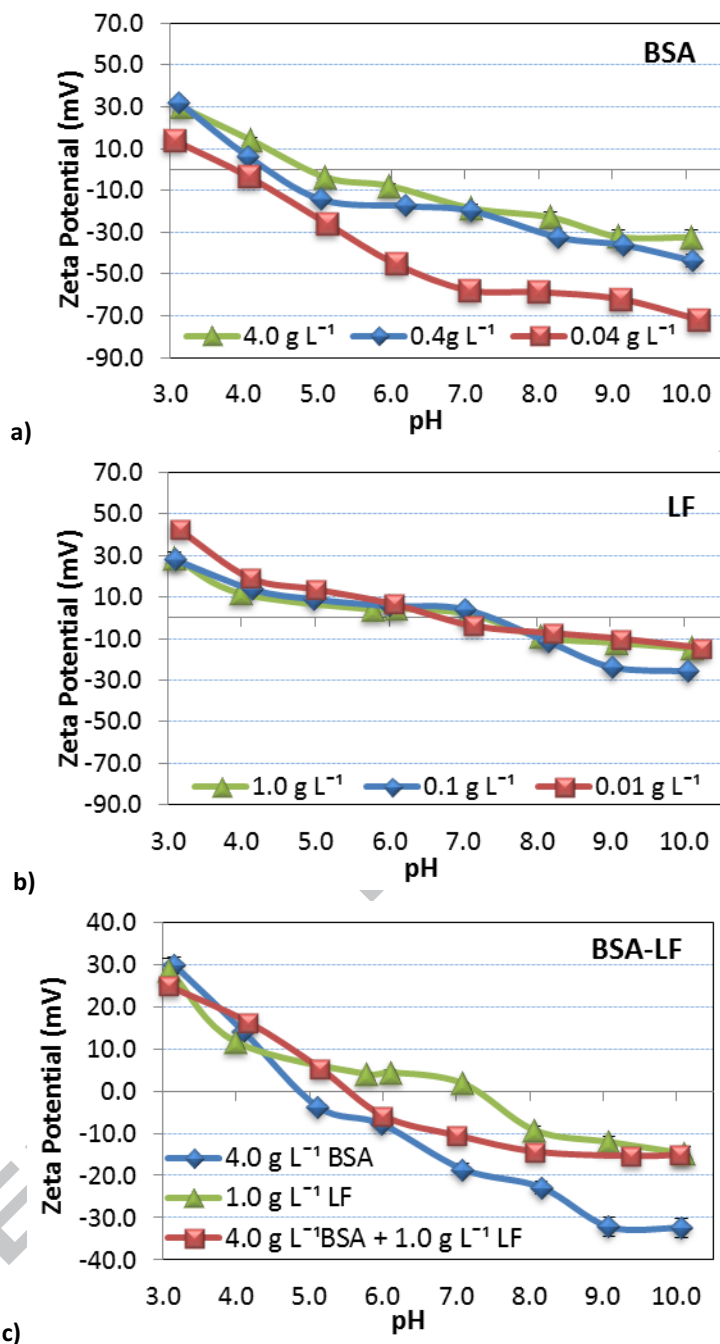
Figure 3. Change in zeta potential with pH for different protein concentrations using 0.025 M KCl: a) BSA, b) LF and c) BSA-LF mixtures.

As shown in Figure 3a, the decrease in protein concentration in the case of BSA was translated into an increase in the absolute value of the zeta potential and a decrease in the isoelectric point, which changed from 4.9 to 3.9 in the studied range of protein concentrations. This behavior is consistent with the decrease of electrophoretic mobility when increasing the

10

concentration reported by Ho et al., 2000 [26]. However, in the case of LF, the decrease in the protein concentration (Figure 3b) did not lead to significant changes in the zeta potential behavior. Figure 3c shows that the zeta potential of the protein mixture exhibited an intermediate behavior between both individual curves but different from the expected result according to the concentration ratio of the proteins.

The highest difference of zeta potential between both proteins working with KCl 0.025 M was observed for lowest concentration of the proteins studied (0.04 g L^{-1} for BSA and 0.01 g L^{-1} for LF), being the zeta potential -45.0 mV for BSA and 6.7 mV for LF at pH 6.0.

Summarizing, the influence of pH, electrolyte medium and concentration as well as the BSA and LF proteins' concentration has been experimentally determined under different conditions leading to values of the isoelectric point (Ip) of BSA that lie in the range 3.8 - 5.5, whereas for LF, the measured values fall in the range 5.6 - 9.3. Thus, the obtained results highlight the influence of the characteristics of the protein medium on their properties.

3.2. Protein size measurements

Protein separation processes are strongly affected by protein size. Far from being constant, this property is influenced by pH and protein concentration. Here, BSA and LF size values have been determined at different pH (3.0-10.0) and protein concentrations (1.0, 1.0/10.0, 1.0/100.0).

Influence of pH

The effective size of the protein molecules was measured by DLS at different pH values in the range 3.0 to 10.0 using 0.025 M KCl solution and concentrations of 4.0 g L^{-1} for BSA and 1.0 g L^{-}

[1] for LF. Using the CONTIN approximation [27], graphs of intensity distribution versus particle diameter were obtained for both proteins (Figure 4).
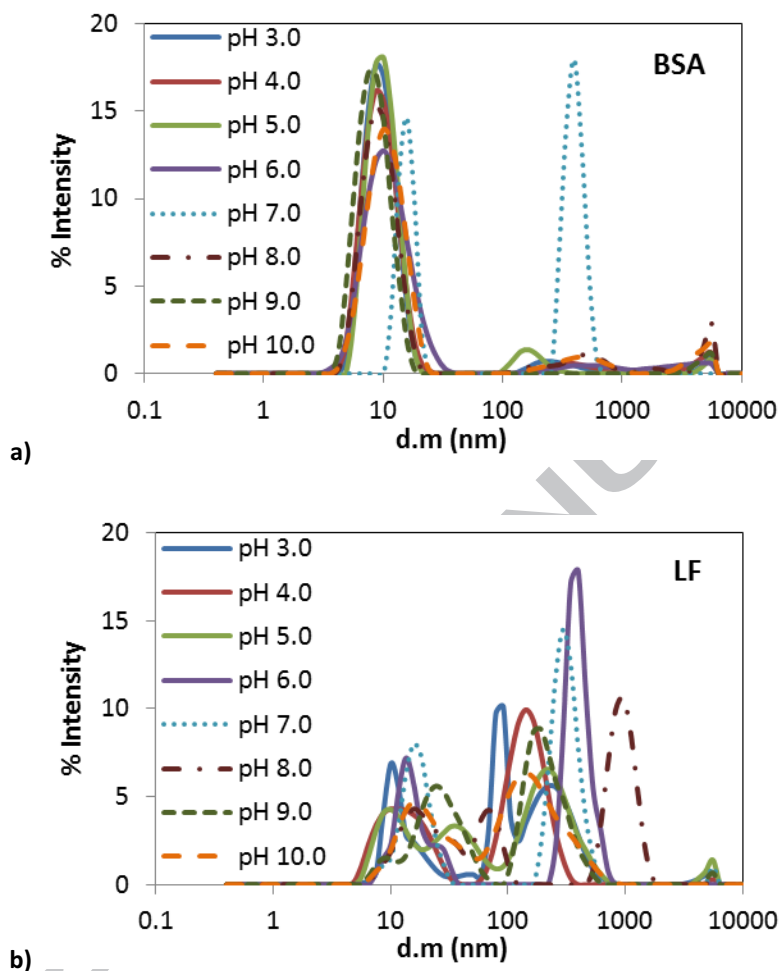
Figure 4. Intensity-size distribution at different pH: a) 4.0 g L^{-1} BSA and b) 1.0 g L^{-1} LF.

BSA samples (Figure 4a) exhibited almost monomodal and stable curves (with the exception of pH 7.0); for this reason, the z-average size can be considered the hydrodynamic size. Conversely, the LF intensity distribution showed a polydisperse behavior. Thus, it is necessary to study the particle volume distribution for the correct analysis of the data and the proper determination of the hydrodynamic size.

Visually, the polydisperse intensity curves for LF (Figure 4b) suggest the presence of aggregates. The broad peak shape in the case of BSA (Figure 4a) may be caused by the presence of

some aggregates, which will be confirmed with the polydispersity index (PdI) analysis (see Appendix A). The intensity distribution analysis is extremely sensitive to changes in size and aggregation. This highlights that DLS is a powerful technique for detecting the presence of very small numbers of relatively large particles, which can provide an early indication of the stability issues during protein storage or during separation processes [27].

The z-average size of BSA versus pH is plotted in Figure 5a. It shows that there was no significant change with pH, except at the Ip value. This result is consistent with the behavior found in many protein solutions where reversible aggregation under nondenaturing (no temperature or pressure applied) conditions is most readily observed at pHs close to the isoelectric point [28]. Figure 5b presents the change in PdI with pH for this protein; most of the values lie above the recommended PdI value (0.2), suggesting the presence of oligomers and/or aggregates.

a)

b)

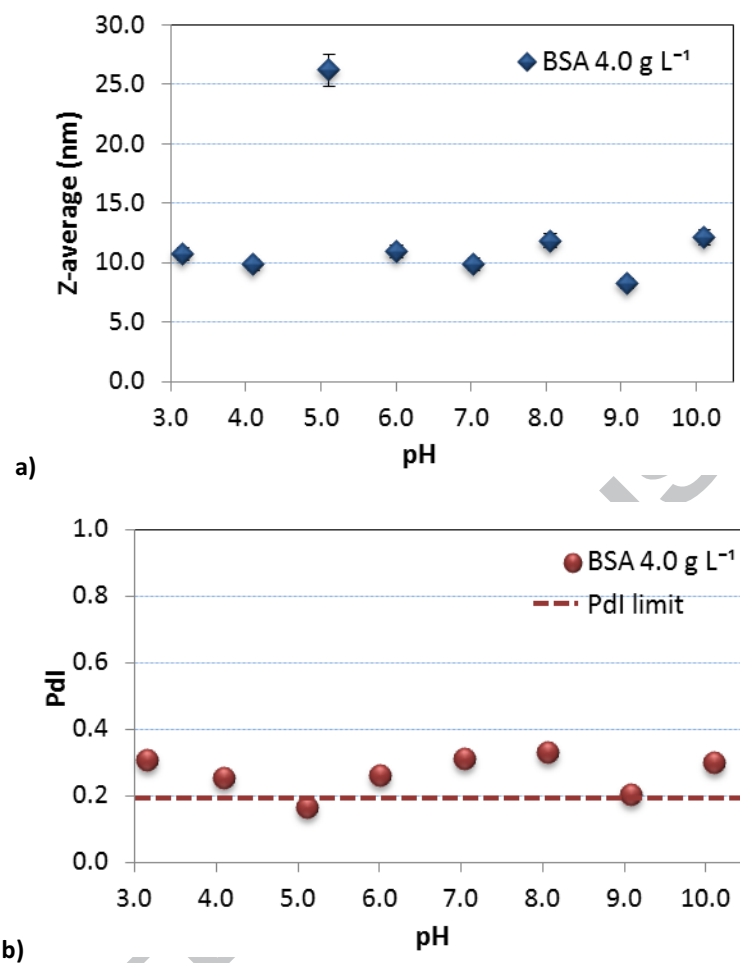**Figure 5. Change in a) Z-average size and b) PdI for 4.0 g L^{-1} of BSA at 0.025 M KCl and different pHs.**

Figure 6 depicts the size of both proteins through the volume/mass distribution using the

values tabulated Tables 1-6C of Appendix C.
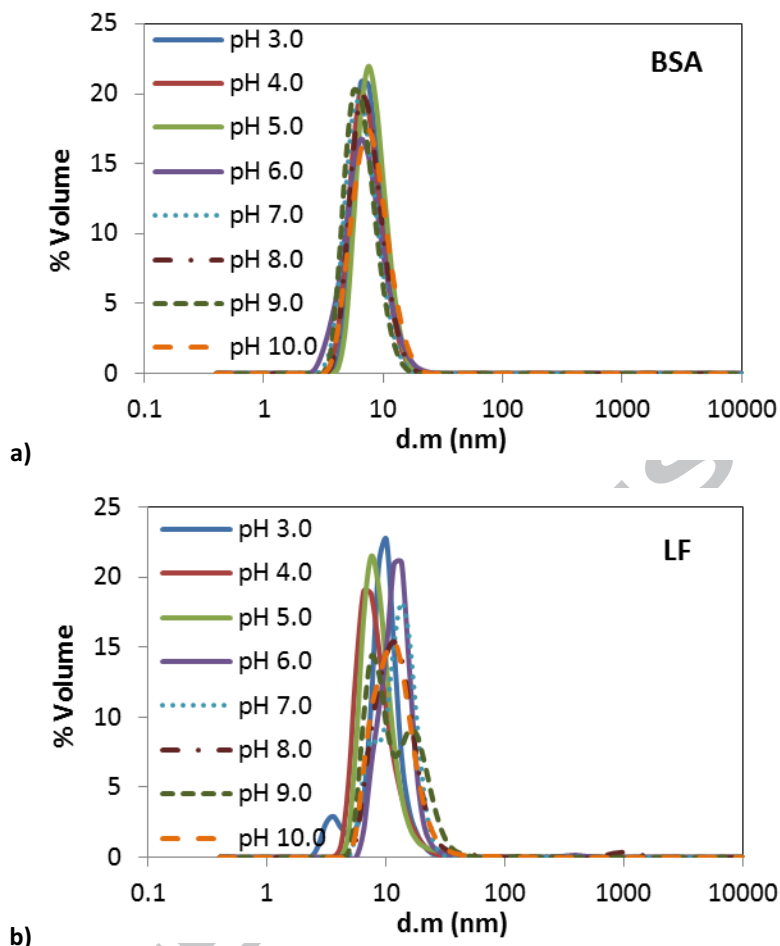
Figure 6. Volume distribution: a) 4.0 g L^{-1} BSA and b) 1.0 g L^{-1} LF.

The accurate particle size value is the average value of the volume distribution with size because of the contribution of at least 90 % of each peak to the total volume of the sample [29]. Figure 6 shows that there is no significant influence of pH on the hydrodynamic diameter of BSA, which has an average value of 7.5 nm. However, there is a tendency for LF to increase in size from pH 4.0 to pH 7.0 (8.5-12.3 nm) and slightly decrease in size from pH 8.0 to pH 9.0 (12-8.9 nm). At pH 3.0, this protein exhibits an intermediate behavior (10.2 nm). Nevertheless, there is not a large difference, as all the values fell in the range between 8.5 nm and 12.3 nm.

The hydrodynamic diameter and molecular weight values lead to the conclusion that BSA samples show no aggregation while a percentage in mass from 0.2-4.0% of aggregates is found in

the LF samples. The tables with the data of mean size with its standard deviation, mass percentage, estimated molecular weight and the %Pd are included in Appendix C.

As the separation of BSA/LF by ultrafiltration is influenced not only by the zeta potential but also by the protein size, maximum differences between the sizes of both proteins are required. Under the experimental conditions, the highest difference in molecular size between both proteins was observed at pH 7.0 being BSA and LF molecular sizes 6.9 nm and 14.3 nm, respectively.

Influence of protein concentration

The change in hydrodynamic diameter of the proteins with pH was measured for the following concentration ranges: 0.04-4.0 g L^{-1} for BSA and 0.01-1.0 g L^{-1} for LF. The mixture of 4.0 g L^{-1} of BSA and 1.0 g L^{-1} of LF was also studied. Hawe et al., 2011 [17] note that increases in protein concentration result in a reduction in the measured size of the protein, but there is a lack of information in the literature about the average molecular size of protein mixtures.
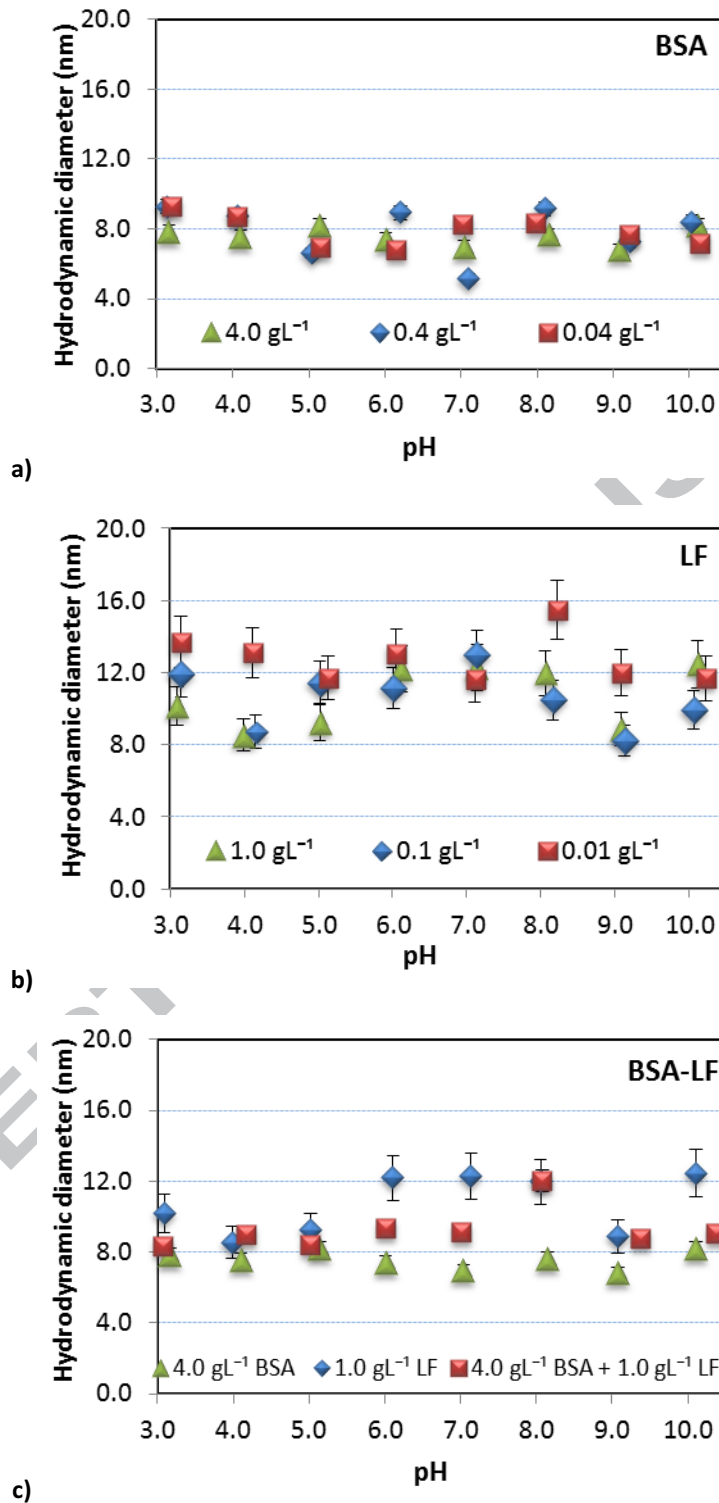
a)

b)

c)

Figure 7. Change in protein molecular size with pH for different protein concentrations: a) BSA, b) LF and c) protein mixtures at 0.025 M KCl.

Figure 7 shows that there was no influence of either the protein concentration or the pH on the protein size of BSA (almost all values fell between 7.0 and 9.2 nm, with the average hydrodynamic size previously determined of 7.5 nm (4.0 g L^{-1} BSA)). The hydrodynamic size of LF showed a similar behavior with pH for 0.1 g L^{-1} and 1.0 g L^{-1} LF solutions (with the exception of pH 10.0), with values that fall between 8.0 nm and 12.0 nm, but as the protein concentration decreased (0.01 g L^{-1}), the hydrodynamic diameter increased (values between 11.5 nm and 15.0 nm). These results are in agreement with those reported previously by other authors who described an increase in the protein molecular size with decreasing concentration [17]. Although increases in the protein concentration commonly result in an increase in protein aggregation [7,27], some authors consider the opposite behavior due to the repulsion-attraction forces. The increase in concentration reduces the attraction forces, resulting in decreased protein-protein interactions and therefore the formation of aggregates [30].

With regard to the mixture values, as one of the proteins was much more concentrated than the other, the expected change was closer to the more concentrated protein (BSA), but the experimental data showed an intermediate behavior, with the exception of the values corresponding to both isoelectric points, for which the mixture exhibited the same hydrodynamic diameter as the neutral protein.

The highest difference in molecular size was found at the set of conditions, pH 6.0 and 0.04 g L^{-1} for BSA and 0.01 g L^{-1} for LF, being the sizes 6.8 nm and 13.0 nm for BSA and LF, respectively.

In conclusion the protein size is strongly affected by the medium characteristics, especially in the case of LF, where a significant formation of dimers has been shown. This behavior could be

18

determinant in the selection of the conditions that favor the separation of the considered proteins.

3.3. Comparison between experimental and calculated data and values reported in literature

Isoelectric points

The direct comparison of the measured zeta potential data and the theoretical protein charge is difficult because of the lack of knowledge about the double layer thickness. The point where both (theoretical and experimental) data match is the isoelectric point. Theoretical Ips were determined by means of equations B2-B7 (Appendix B). The obtained values are collected in Table 1.

Table 1. Experimental, calculated and literature values of Isoelectric Point for BSA and LF proteins.

BSA Protein		Isoelectric point (Ip)		
Medium	Concentration (g L^{-1})	Measured	Calculated	Literature
KCl 0.01 M	4.0	5.0	5.0	4.7[a]
NaCl 0.01 M		5.1	5.0	5.1[c]
CaCl$_2$ 0.01 M		5.5	4.9	4.7[a]
KCl 0.025 M		4.9	4.9	---
KCl 0.05 M		4.9	4.8	---
KCl 0.1 M		4.7	4.8	4.7[e]
KCl 0.025 M	0.4	4.4	4.9	4.7[a]
	0.04	3.9	4.9	5.1[g]
LF Protein		Isoelectric point (Ip)		
Medium	Concentration (g L^{-1})	Measured	Calculated	Literature
KCl 0.01 M	1.0	9.3	9.5	9.0[b]
NaCl 0.01 M		9.2	9.5	---
CaCl$_2$ 0.01 M		9.4	9.3	---
KCl 0.025 M		7.3	9.3	7.2[d]
KCl 0.05 M		6.0	9.1	---
KCl 0.1 M		5.7	8.9	5.6[f]
KCl 0.025 M	0.1	7.3	9.3	---
	0.01	6.7	9.3	---

*4.0 g L^{-1} of BSA or 1.0 g L^{-1} of LF; +0.025 M KCl; [a]0.5 g L^{-1} BSA in 0.001 M KCl, NaCl, or CaCl$_2$ [31]; [b]0.1 g L^{-1} LF in 0.01 M KCl [24]; [c]1 g L^{-1} BSA in 0.01 M NaCl [15]; [d]0.2 g L^{-1} LF in 0.01 M NaCl [25]; [e]0.5 g L^{-1} BSA in 0.1 M KCl [16]; [f]0.4 g L^{-1} LF in 0.15 M NaCl [12]; [g]0.006 g L^{-1} BSA in NaCl [32].

As seen in Table 1, the theoretical and experimentally determined isoelectric points of BSA are in agreement and are similar to previously reported values in the literature. However, for LF the experimental results at high electrolyte concentrations deviate considerably from the theoretical data (5.6 - 7.3 for the measured values in contrast to 8.9 - 9.3 for the calculated values). Although the literature provides few data of this protein, most of the values already reported are in agreement with those experimentally measured in this work.

Protein size and qualitative analysis of aggregates

The calculated Stokes (or hydrodynamic) diameter determined by equation (B8) (Appendix B) were compared to the experimental size (Figure 8).
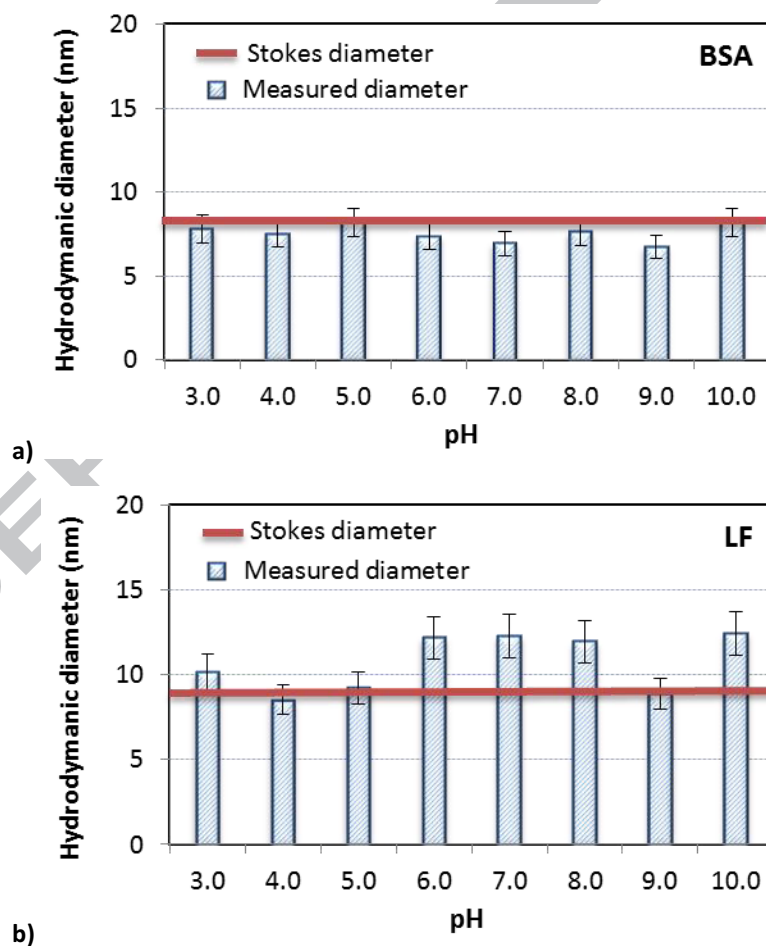
Figure 8. Comparison of the change in the calculated and measured protein molecular size with pH at 0.25 M ionic strength: a) BSA and b) LF.

Figure 8a shows the similarity between the calculated and experimentally determined diameters. Measured diameters are close to the value of Stokes diameter (6.9 nm) and within the values of the experimental error. This behaviour agrees with the fact that the % PdI value (see Appendix A) is close to the standard value for aggregation (28.0 % PdI). The slight difference in the measured and calculated values of BSA molecular weight is attributed to the hypothesis of spherical shape molecules assumed in the zetasizer software (Table 1C). Measured diameters of LF are higher than Stokes diameter, Figure 3.8b, mainly due to the formation of aggregates as shown in Table 4C

3.4. Selection of the most suitable experimental conditions

Taking into account the results previously obtained, Figure 9 collects the summary of the best experimental conditions to improve the efficiency of BSA/LF proteins separation using charged ultrafiltration membranes [3].

Figure 9. Experimental conditions for the separation of BSA and LF proteins.

Figure 9 shows the best experimental conditions tested in this work for the separation BSA/LF mixtures using charged ultrafiltration membranes. Working with positively charged membranes the isolation of BSA from a mixture of 0.04 g L^{-1} of BSA and 0.01 g L^{-1} of LF might be achieved employing 0.025M KCl at pH 6.0. The separati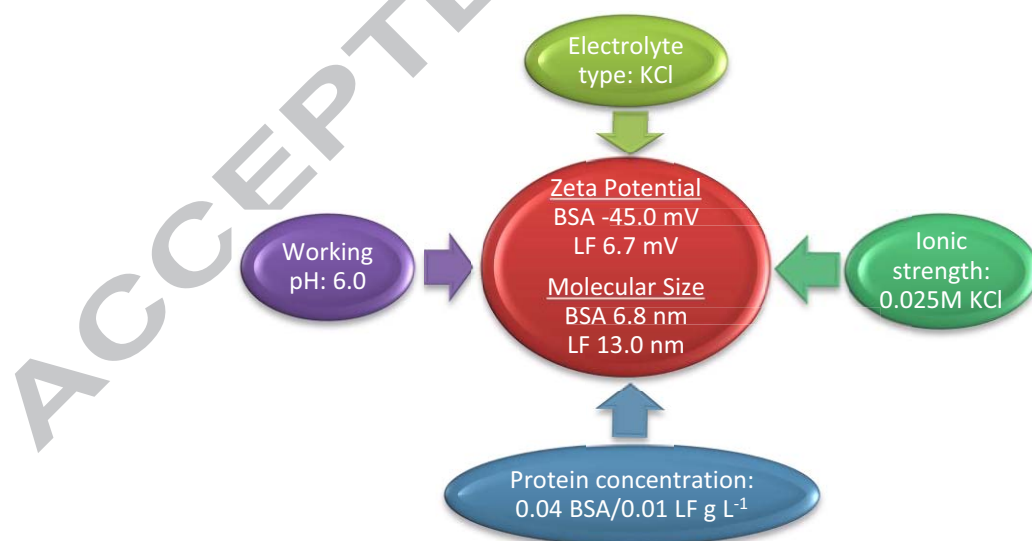on is promoted by the difference of the sizes between both proteins and the repulsion of the positively charged LF protein by the positively charged membrane. Working with negatively charged membranes the isolation of LF from a mixture of 0.04 g L^{-1} of BSA and 0.01 g L^{-1} of LF can be achieved employing 0.025M KCl at pH 6.0. The separation is promoted by the repulsion of the negatively charged BSA protein by the negatively charged membrane.

5. Conclusions

This paper reports theoretical and experimental data on the changes in protein size, isoelectric point and zeta potential with pH for BSA and LF (individually and as a mixture) under different experimental conditions, including the solution ionic strength, electrolyte type and concentration and protein concentration.

With regard to the zeta potential, the ionic strength and protein concentration showed a significant influence on this parameter, whereas the electrolyte type showed only slight influence on zeta potential. The measured isoelectric points (Ip) of BSA were in the range 3.8 - 5.5, whereas for LF, the measured values were in the range 5.7 - 9.3. These values are far different from the theoretical predictions. The maximum difference in the charge of BSA and LF was obtained in the range of pH between 5.0 and 6.0 for the studied experimental conditions.

With regard to the protein molecular size, the pH and protein concentration did not appear to have a significant influence. The average size for BSA was determined to be 7.8 $\pm$ 1.0 nm, whereas for LF, the average size was found to be 10.65 $\pm$ 0.65 nm in the protein concentration range 0.01 - 0.1 g L^{-1} and 12.8 $\pm$ 0.8 nm for 1.0 g L^{-1}. The highest difference in size between BSA

22

and LF was obtained at pH 7.0 while the lowest polydispersity index values of both proteins were determined at pH 9.0.

The results obtained were compared to theoretical values and a significant deviation was observed under the specific conditions of this study. This deviation was most likely due to the formation of aggregates not predicted in theory or by the simplicity of the assumptions used in the theoretical descriptions. Thus, the availability of accurate parameters is necessary to correctly design protein separation and purification processes. The most suitable conditions for the proteins separation by electrophoretic mobility or size exclusion have been selected.

The results of this work highlight the relevance of the determination and use of reliable experimental data that will maximize the effectiveness of the separation processes of high added value food proteins, increasing the knowledge of the physicochemical interactions between protein molecules, which are guided by their electric surface properties.

Acknowledgments

References

[1] C. Schmitt, C. Bovay, A.-M. Vuilliomenet, M. Rouvet, L. Bovetto, R. Barbar, et al., Multiscale characterization of individualized beta-lactoglobulin microgels formed upon heat treatment under narrow pH range conditions, Langmuir. 25 (2009) 7899–909.
[2] J. Baró, L. Jiménez, L.J., Martínez-Pérez, A. and Bouza, Péptidos y proteínas de la leche con propiedades funcionales, Ars Pharm. 42 (2001) 135–145.
[3] V. Valiño, M.F. San Román, R. Ibañez, I. Ortiz, Improved separation of bovine serum albumin and lactoferrin mixtures using charged ultrafiltration membranes, Sep. Purif. Technol. 125 (2014) 163–169.
[4] O. Shinkazh, D. Kanani, M. Barth, M. Long, D. Hussain, A.L. Zydney, Countercurrent tangential chromatography for large-scale protein purification., Biotechnol. Bioeng. 108 (2011) 582–91.
[5] J. Cheng, Y. Li, T.S. Chung, S.-B. Chen, W.B. Krantz, High-performance protein separation by ion exchange membrane partitioned free-flow isoelectric focusing system, Chem. Eng. Sci. 63 (2008) 2241–2251.

[6] A. Saxena, B.P. Tripathi, M. Kumar, V.K. Shahi, Membrane-based techniques for the separation and purification of proteins: an overview, Adv. Colloid Interface Sci. 145 (2009) 1–22.

[7] H.-C. Mahler, W. Friess, U. Grauschopf, S. Kiese, Protein aggregation: pathways, induction factors and analysis, J. Pharm. Sci. 98 (2009) 2909–34.

[8] N.S. Pujar, A.L. Zydney, Electrostatic and electrokinetic interactions during protein transport through narrow pore membranes, Ind. Eng. Chem. Res. 33 (1994) 2473–2482.

[9] W.R. Bowen, P.M. Williams, Quantitative predictive modelling of ultrafiltration processes: colloidal science approaches, Adv. Colloid Interface Sci. 134-135 (2007) 3–14.

[10] M.F. Drenski, M.L. Brader, R.W. Alston, W.F. Reed, Monitoring protein aggregation kinetics with simultaneous multiple sample light scattering, Anal. Biochem. 437 (2013) 185–97. [11] Y.-I. Lim, S.B. Jørgensen, I.-H. Kim, Computer-aided model analysis for ionic strength-dependent effective charge of protein in ion-exchange chromatography, Biochem. Eng. J. 25 (2005) 125–140.

[12] I. Mela, E. Aumaitre, A.-M. Williamson, G.E. Yakubov, Charge reversal by salt-induced aggregation in aqueous lactoferrin solutions, Colloids Surf. B. Biointerfaces. 78 (2010) 53–60.

[13] B.E. Dybowska, Properties of milk protein concentrate stabilized oil-in-water emulsions, J. Food Eng. 88 (2008) 507–513.

[14] A.R. Jambrak, T.J. Mason, V. Lelas, L. Paniwnyk, Z. Herceg, Effect of ultrasound treatment on particle size and molecular weight of whey proteins, J. Food Eng. 121 (2014) 15–23.

[15] A. Salis, M. Boström, L. Medda, F. Cugia, B. Barse, D.F. Parsons, et al., Measurements and theoretical interpretation of points of zero charge/potential of BSA protein, Langmuir. 27 (2011) 11597–604.

[16] S. Salgin, U. Salgin, S. Bahadir, Zeta potentials and isoelectric points of biomolecules: the effects of ion types and ionic strengths, Int. J. Electrochem. Sci. 7 (2012) 12404–12414.

[17] A. Hawe, W.L. Hulse, W. Jiskoot, R.T. Forbes, Taylor dispersion analysis compared to dynamic light scattering for the size analysis of therapeutic peptides and proteins and their aggregates, Pharm. Res. 28 (2011) 2302–2310.

[18] M.P. Mier, R. Ibañez, I. Ortiz, Influence of process variables on the production of bovine milk casein by electrodialysis with bipolar membranes, Biochem. Eng. J. 40 (2008) 304–311.

[19] E. Alvarez-Guerra, A. Irabien, Extraction of lactoferrin with hydrophobic ionic liquids, Sep. Purif. Technol. 98 (2012) 432–440.

[20]   C. Tanford, S.A. Swanson, W.S. Shore, Hydrogen ion equilibria of bovine serum albumin, J. Am. Chem. Soc. 77 (1955) 6414–6421. http://dx.doi.org/10.1021/ja01629a002 (accessed April 10, 2014).

[21] G. Scatchard, Y.V. Wu, A.L. Shen, Physical chemistry of protein solutions. X. The binding of small anions by serum albumin, J. Am. Chem. Soc. 81 (1959) 6104–6109.

[22] M. Cappelezzo, C.A. Capellari, S.H. Pezzin, L.A.F. Coelho, Stokes-Einstein relation for pure simple fluids, J. Chem. Phys. 126 (2007) 224516.

[23] B. Jachimska, M. Wasilewska, Z. Adamczyk, Characterization of globular protein solutions by dynamic light scattering, electrophoretic mobility, and viscosity measurements, Langmuir. 24 (2008) 6866–72.

[24] M. Nyström, P. Aimar, S. Luque, M. Kulovaara, S. Metsämuuronen, Fractionation of model proteins using their physiochemical properties, Colloids Surfaces A Physicochem. Eng. Asp. 138 (1998) 185–205.

[25] N. Ndiaye, Y. Pouliot, L. Saucier, L. Beaulieu, L. Bazinet, Electroseparation of bovine lactoferrin from model and whey solutions, Sep. Purif. Technol. 74 (2010) 93–99.

[26] A. Ho, J. Perera, G. Stevens, The effect of protein concentration on electrophoretic mobility, J. Colloid Interface Sci. 224 (2000) 140–147.

[27] M.J. Treuheit, A.A. Kosky, D.N. Brems, Inverse relationship of protein concentration and aggregation, Pharm. Res. 19 (2002) 511–516.

[28] M.G. Carneiro-da-Cunha, M.A. Cerqueira, B.W.S. Souza, J.A. Teixeira, A.A. Vicente, Influence of concentration, ionic strength and pH on zeta potential and mean hydrodynamic diameter of edible polysaccharide solutions envisaged for multinanolayered films production, Carbohydr. Polym. 85 (2011) 522–528.

[29] L.S. Yu, G.L. Yang, Z.J. He, Y.F. Li, Iterative CONTIN algorithm for particle sizing in dynamic light scattering, Guangdian Gongcheng/Opto-Electronic Eng. 33 (2006) 64–69.

[30] P.R. Majhi, R.R. Ganta, R.P. Vanam, E. Seyrek, K. Giger, P.L. Dubin, Electrostatically driven protein aggregation: beta-lactoglobulin at low ionic strength, Langmuir. 22 (2006) 9150–9159.

[31] F. Zhang, M.W.A. Skoda, R.M.J. Jacobs, R.A. Martin, C.M. Martin, F. Schreiber, Protein interactions studied by SAXS: effect of ionic strength and protein concentration for BSA in aqueous solutions, J. Phys. Chem. B. 111 (2007) 251–9.

[32] Y. Mukai, E. Iritani, T. Murase, Effect of protein charge on cake properties in dead-end ultrafiltration of protein solutions, J. Memb. Sci. 137 (1997) 271–275.

[33] R.J. Hunter, Zeta potential in colloid science: principles and applications, 2nd Ed, Academic Press, London, UK, 1981.

[34] C. Unterhaslberger, G. ; Schmitt, C. ; Shojaei-Rami, S. ; Sanchez, Beta-Lactoglobulin Aggregates from Heating with Charged Cosolutes: Formation, Characterization and Foaming, in: E. Dickinson, M.E. Leser (Eds.), Food Colloids Self-Assembly Mater. Sci., 1st Ed, Royal Society of Chemistry, Cambridge, UK, 2007: p. 18.

[35] Malvern, Zetasizer user manual, http://www.malvern.com. (2013).

[36] M. Kaszuba, J. Corbett, F.M. Watson, A. Jones, High-concentration zeta potential measurements using light-scattering techniques, Philos. Trans. 368 (2010) 4439–51.

[37] V.M. Starov, Nanoscience: colloidal and interfacial aspects, 1st Ed, CRC Press, Boca Raton, Florida, USA, 2011.

[38] Z. Adamczyk, M. Nattich, M. Wasilewska, M. Zaucha, Colloid particle and protein deposition - electrokinetic studies, Adv. Colloid Interface Sci. 168 (2011) 3–28.

[39] S. Rao, A.L. Zydney, High resolution protein separations using affinity ultrafiltration with small charged ligands, J. Memb. Sci. 280 (2006) 781–789.

[40] B.J. Compton, Electrophoretic mobility modeling of proteins in free zone capillary electrophoresis and its application to monoclonal antibody microheterogeneity analysis, J. Chromatogr. A. 559 (1991) 357–366.

[41] C.A. Smith, Estimation of sedimentation coefficients and frictional ratios of globular proteins, Biochem. Educ. 16 (1988) 104–106.

[42] R.M. Parry, E.M. Brown, Protein-metal interactions. lactoferrin conformation and metal binding properties, Adv. Exp. Med. Biol. 48 (1974) 141–160.

Appendix A

Electrophoretic Light Scattering for Zeta Potential Measurements

The zeta potential, determined using the Zetasizer Nano ZS, was obtained by applying the M3-PALS technique and consisted of a combination of laser Doppler velocimetry (LDV) and phase analysis light scattering (PALS). This measurement can be used for particles in the size range from 0.38 nm to 100 μm. In this technique, an electrical field is applied across a pair of electrodes placed at both ends of a DTS1061 disposable folded capillary cell containing the protein solution. Charged particles are attracted by the oppositely charged electrode and the electrophoretic mobility, μ_E, is represented as the velocity of this movement per unit of field. Then, the zeta potential was calculated by the Henry equation [15]:

$$\mu_E = \frac{2\varepsilon\zeta f(\kappa a)}{3\eta} \tag{A1}$$

where ε is the dielectric constant of the medium, ζ the zeta potential, η the viscosity and $f(\kappa a)$ the Henry's function, which is related to the Debye length (κ^{-1}). It was assumed that the double layer thickness is larger than the particle size [33] and the Hückel approximation ($\kappa a < 1$) was used in its calculation where $f(\kappa a) = 1$. Six zeta potential measurements of 11 runs each were performed for every sample. Data shown in figures are average values of the 6 measurements with the relative measurement error.

Dynamic Light Scattering for Protein Size Measurements

Protein size was determined by dynamic light scattering (DLS) using the aforementioned Zetasizer Nano ZS. The apparatus was outfitted with a 4.0 mW power source and with a He-Ne laser emitting at 633.0 nm. The instrument uses a scattering angle of 173.0º for detection using an avalanche photodiode due to a backscattering configuration. The protein solutions (1.0 mL) were placed in DTS0012 square disposable polystyrene cuvettes and measurements were performed at room temperature. The path length of the light was set automatically by the apparatus, taking into account the sample turbidity. The translational diffusion coefficient of the particle (D_{app}) was calculated using the Stokes-Einstein equation from the polynomial fit of the logarithm of the correlation function using the cumulants method [34]:

$$D_{app} = \frac{k\ T}{3\Pi \eta\ d}$$ (A2)

where k is the Boltzmann constant, η is the sample dynamic viscosity, T is the absolute temperature and D_{app} is the diffusion coefficient. The hydrodynamic diameter (d) was obtained by assuming that the diffusing particles were monodisperse spheres. Three measurements of 20 runs each were performed for every sample. The values shown in the figures are the average value of 3 measurements with the relative measurement error.

The molecule size is evaluated from the correlation function by applying several algorithms. Two approaches can be used: (1) the cumulants analysis, which fits the correlation function to a single exponential to obtain an estimate of the width of the distribution (polydispersity index, PdI) and the mean size (z-average diameter), or (2) CONTIN analysis, which follows a multiple exponential fitting to obtain the distribution of protein sizes.

The intensity size distribution is a plot of the relative intensity of light scattered by particles in various size groups. If the distribution by intensity is formed by a single fairly smooth peak (PdI < 0.2), then there is no point in converting it to a volume distribution using the Mie theory. However, if the plot presents an important tail or more than one peak (PdI > 0.2), then the Mie theory can apply the input parameter of the sample refractive index to convert the intensity distribution to a volume distribution. This will then give a more realistic analysis of the importance of the tail or second peak present in the measurement. In general terms, d(intensity) > d(volume) > d(number) [34].

When the sample is dispersed, the PdI value is not an accurate parameter to describe it. The % Pd (width peak*100/mean peak) is more suitable. The limits of this parameter are: lower than 28% monodisperse sample (narrow distribution), higher than this value, polydisperse (broad distribution) [35].

Appendix B

Theoretical charge and molecular size determination

The distribution of ions in the surrounding interfacial region is affected by the development of a net charge at the particle surface, leading to an increased concentration of counter ions (ions of opposite charge) close to the surface. Hence, an electrical double layer forms around each particle. The liquid layer surrounding the particle is formed by two parts: an inner region, where the ions are strongly bound, named the Stern layer (Stern potential) and an outer or diffuse region (diffuse layer), where ions are less strongly attached. The diffuse layer contains a notional boundary inside where the particles and ions form a stable entity. When a particle changes its place (e.g., by gravity or other forces), the ions in the boundary also move with it, but none of the ions beyond the boundary move. This boundary is named the slipping plane or surface of hydrodynamic shear [36]

The potential related to this boundary is known as the Zeta potential (Figure 1B) and its value is a measure of system stability. Particles with large negative or positive zeta potentials are usually considered stable.
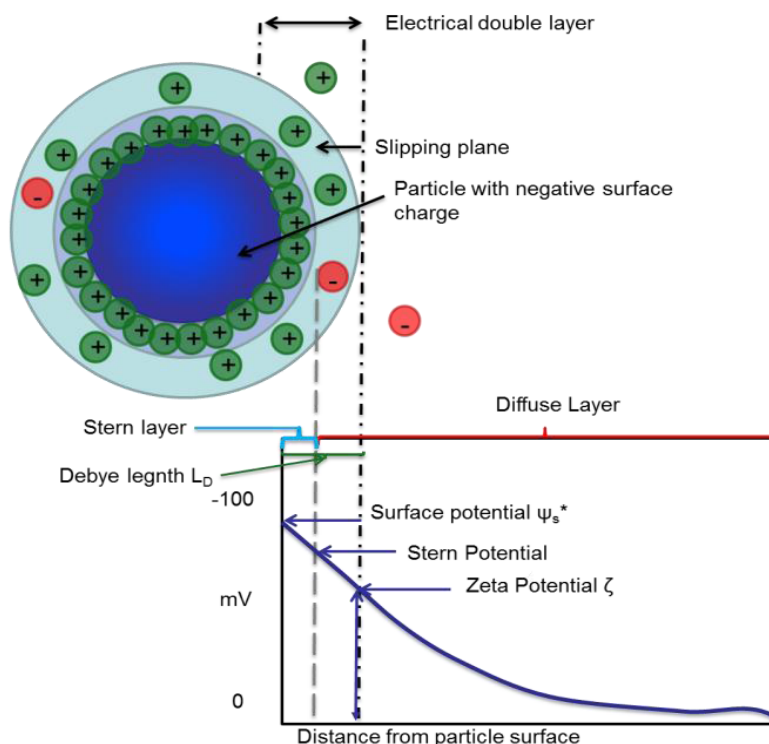
Figure 1B. Schematic picture of the protein charge.

The degree of ionization of a given amino acid is related to the local H$^+$ concentration, which can be represented for a carboxylic acid as:

$$R-COOH \xleftrightarrow{K^{int}} R-COO^- + H^+$$ (B1)

The net protein charge ($Z_{protein}$) was calculated from the difference in the number of protonated amino acids (Z_H^+) and the number of bound anions (Z_{ion}^-):

$$Z_{protein} = Z_{H^+} - Z_{ion^-}$$ (B2)

Proteins are composed of a number of different types of amino acids, but only certain amino acids will participate in the ionization reactions that will form a charge on protein surface. These groups are named the tihtratable amino acids or the charged amino acid residues [9].

The positive charge of the protein is calculated by the expression:

$$Z_{H+} = z_{max} - \sum_i \frac{n_i K_i^{int}}{K_i^{int} + [H_b^+] \exp(-e\psi_s^*/kT)}$$ (B3)

where [H$_b^+$] is the bulk hydrogen ion concentration and the number (n_i) and intrinsic equilibrium constants (K^{int}) for each titratable amino acid (i) are given in Table 1B for BSA [37] and for LF [9]. The total number of positively charged amino acid residues at very low pH, i.e., where all the available sites are protonated, is Z_{max} = 96 for BSA and Z_{max} = 82 for LF.

Table 1B. Type and number of titratable amino acids on BSA and LF

BSA [37]			LF [9]		
Type (i)	Number (n_i)	pK^{int}	Type (i)	Number (n_i)	pK^{int}
a-Carboxyl	1	3.8	Aspartic acid	30	4.7
b,g-Carboxyl	99	4.0	Glutamic acid	34	4.7
Imidazole	16	6.9	Histidine	3	6.5
a-Amino	1	7.7	Lysine	39	10.2
e-Amino	57	9.8	Tyrosine	10	9.9
Phenolic	19	10.3	Arginine	30	12.0
Guanidine	22	12.0			
	$Z_{max} = 96$			$Z_{max} = 82$	

The equations (B1-B3) consider a single globular protein encircled by a solution of positively charged cations and negatively charged anions. The proteins radii were estimated as 35 Å for BSA [37] and 30 Å for LF [9]. The electrostatic potential is averaged over the spherical surface on the model protein surface. However, on a real protein, charges are localized and there will easily be local variations in charge density and there will be counterions clustering at the charged group. Nevertheless, it has been demonstrated that this simplified model can qualitatively explain many trends in protein solutions [15].

The Boltzmann factor is the exponential term in equation (B3) and accounts for the partitioning of the hydrogen ions due to electrostatic interactions into the region immediately adjacent to the protein surface. Hence, the H^+ concentration close to a negatively charged protein will be higher than the bulk value. ψ_s^* is the electrostatic potential at the protein surface and its relationship with the net protein charge can be described as [9]:

$$\sigma_s^* = \frac{\varepsilon_0\,\varepsilon\,\psi_s^*(1+\kappa\,r_s)}{r_s} = \frac{e\,Z_{protein}}{4\Pi\,r_s^2} \tag{B4}$$

where r_s is the solute radius of the BSA or LF, e is the electron charge, ε_0 is the permittivity of free space, ε is the dielectric constant of the medium and κ is the inverse of the Debye length (L_D) [38]:

$$\kappa = \sqrt{\left(\frac{F^2}{\varepsilon_0\varepsilon\,RT}\right)\sum z_i^2 C_i} = \frac{1}{L_D} \tag{B5}$$

In equation (B5), *F is* Faraday's constant, R is the gas constant, T the absolute temperature, z the valence and C_i the concentration of each ion.

The number of bound ions was calculated in a similar way as (Teixera et al., 2010):

$$Z_{ion^-} = \sum_j \frac{m_j K_j \gamma\left[Ion^-\right]\exp(e\,\psi_s^*/kT)}{1+K_j\gamma\left[Ion^-\right]\exp(e\,\psi_s^*/kT)} \tag{B6}$$

As chloride salts are the most common electrolytes in protein separation processes, the influence of this anion was studied. The parameters m_j and K_j for the three distinct Cl^- binding sites are given in Table 2B [39]. k is the Boltzmann constant and γ is the activity coefficient of the ion, which was obtained as:

$$-\log \gamma = \frac{0.5\sqrt{[Ion^-]/2}}{\left(1 + 2\sqrt{[Ion^-]/2}\right)}$$

(B7)

Table 2B. Values of parameters mj and Kj in the Cl⁻ binding model

J	m_j	K_j (M^{-1})
1.0	1.0	2400.0
2.0	8.0	100.0
3.0	18.0	3.3

The theoretical net protein charge in a given solution was evaluated by simultaneously solving equations from B2 to B7.

To obtain theoretical protein size data, the equation (B8) proposed by Compton (1991) [40] was used. Compton (1991) [40] describe the Stoke's radius of the protein in terms of the more useful, but in fact the more approximate, protein mass through the equation:

$$r = \left(\frac{3M_w v}{4\Pi N}\right)^{1/3}\left(\frac{f}{f_0}\right)$$

(B8)

where f/f_0 is the frictional ratio which can be defined as the ratio the frictional coefficient (f) experienced by the molecule when sedimenting to the theoretical frictional coefficient (f_0) for an ideal sphere of corresponding molecular weight. Thus, the frictional ratio of an ideal sphere would be 1.0. Deviations from this value indicate increasing asymmetry or hydration of the molecule [41]. This parameter is 1.3 for BSA (Sigma technical specifications) and 1.4 for LF [42]. The partial specific volume (v) is 0.734 cm^3 g^{-1} for BSA [40] and 0.723 cm^3 g^{-1} for LF [42]. M is the molecular weight of each protein (BSA=65.0 kDa and LF=78.0 kDa) and N is Avogadro's number (6.022×10^{23} mol^{-1}).

Appendix C

Volume distribution of proteins

The mean size with its standard deviation, percent of each peak in volume/mass, the estimated molecular weight and the %Pd of each peak are shown in the following Tables (C1-C6) for both proteins at the different concentrations and pHs.

Table 1C. Values of PdI, % of peak and mean size for 4.0 g L^{-1} BSA at different pHs.

pH	Peak	Size (nm)	% Mass	kDa estimated	% Pd
BSA 4.0 g L^{-1} Electrolyte: 0.025M KCl
3	1	7.8 ± 2.5	100.0	105.6	28.5
	2	146.5 ± 39.8	0.0	284000.0	25.2
	3	0.00	0.0	0.0	0.0
4	1	7.7± 2.5	100.0	105.6	31.8
	2	902.0 ± 109.5	0.0	565000.0	29.8
	3	0.0	0.0	0.0	0.0
5	1	8.4 ± 2.2	100.0	148.8	26.1
	2	86.0 ± 20.5	0.0	101000.0	17.4
	3	0.0	0.0	0.0	0.0
6	1	7.4 ± 3.3	100.0	105.6	39.5
	2	694.2 ± 302.8	0.0	1120000.0	50.6
	3	0.0	0.0	0.0	0.0
7	1	6.9 ± 2.7	100.0	105.6	31.4
	2	209.0 ± 96.1	0.0	1580000.0	30.6
	3	0.0	0.0	0.0	0.0
8	1	7.3 ± 2.6	100.0	105.6	29.9
	2	267.8 ± 130.3	0.0	565000.0	29.9
	3	0.0	0.0	0.0	0.0
9	1	6.7 ± 1.9	100.0	74.9	29.9
	2	2426.0 ± 541.5	0.0	385000000.0	14.4
	3	0.0	0.0	0.0	0.0
10	1	8.2 ± 2.8	100.0	148.8	33.1
	2	891.9 ± 222.9	0.0	1120000.0	32.0
	3	0.0	0.0	0.0	0.0

Table 2C. Values of PdI, % of peak and mean size for 0.4 g L^{-1} BSA at different pHs.

pH	Peak	Size (nm)	% Mass	kDa estimated	% Pd
		BSA 0.4g L^{-1} Electrolyte: 0.025M KCl			
3	1	8.2 ± 1.5	100.0	148.8	14.1
	2	341.0 ± 42.5	0.0	565000.0	4.2
	3	0.0	0.0	0.0	0.0
4	1	8.7 ± 2.6	99.9	148.8	26.5
	2	543.3 ± 112.7	0.0	401000.0	29.0
	3	0.0	0.0	0.0	0.0
5	1	6.6 ± 1.8	100.0	74.9	23.5
	2	201.4 ± 34.9	0.0	202000.0	16.8
	3	0.0	0.0	0.0	0.0
6	1	8.9 ± 2.3	99.9	148.8	22.3
	2	570.5 ± 136.4	0.1	1580000.0	23.6
	3	0.0	0.0	0.0	0.0
7	1	5.2 ± 1.0	100.0	53.1	9.4
	2	0.0	0.0	0.0	0.0
	3	0.0	0.0	0.0	0.0
8	1	9.2 ± 2.4	99.9	148.8	22.9
	2	531.2 ± 157.5	0.1	72000.0	27.1
	3	0.0	0.0	0.0	0.0
9	1	7.3 ± 1.7	100.0	74.9	22.4
	2	224.9 ± 34.8	0.0	202000.0	21.0
	3	0.0	0.0	0.0	0.0
10	1	8.4 ± 2.2	100.0	105.6	25.5
	2	226.3 ± 88.9	0.0	284000.0	22.0
	3	0.0	0.0	0.0	0.0

32

Table 3C. Values of PdI, % of peak and mean size for 0.04 g L^{-1} BSA at different pHs.

pH	Peak	Size (nm)	% Mass	kDa estimated	% Pd
		BSA 0.04g L^{-1} Electrolyte: 0.025M KCl			
3	1	9.3 ± 1.2	99.9	148.8	11.5
	2	173.5 ± 32.7	0.1	284000.0	11.6
	3	0.0	0.0	0.0	0.0
4	1	8.5 ± 1.4	98.7	105.6	12.7
	2	43.2 ± 5.3	1.0	12900.0	12.2
	3	367.9 ± 61.7	0.3	796000.0	12.9
5	1	6.9 ± 1.5	99.9	74.9	18.3
	2	458.7 ± 94.5	0.1	1120000.0	20.5
	3	0.0	0.0	0.0	0.0
6	1	6.8 ± 2.5	99.8	74.9	26.5
	2	396.1 ± 128.8	0.1	796000.0	23.3
	3	0.0	0.0	0.0	0.0
7	1	8.2 ±2.1	99.9	148.8	21.3
	2	367.9 ±103.2	0.0	565000.0	20.1
	3	0.0	0.0	0.0	0.0
8	1	8.3 ± 1.8	99.8	105.6	22.4
	2	46.7 ± 9.0	0.1	6500.0	16.5
	3	368.8 ± 74.4	0.1	565000.0	17.5
9	1	7.6 ± 1.2	100.0	105.6	13.8
	2	140.3 ± 24.6	0.0	565000.0	10.1
	3	0.0	0.0	0.0	0.0
10	1	7.1 ± 2.0	99.9	74.9	22.2
	2	321.9 ± 100.9	0.1	284000.0	20.6
	3	0.0	0.0	0.0	0.0

Table 4C. Values of PdI, % of peak and mean size for 1.0 g L^{-1} LF at different pHs.

pH	Peak	Size (nm)	% Mass	kDa estimated	% Pd
		LF 1.0 g L^{-1} Electrolyte: 0.025M KCl			
3	1	10.2 ± 3.2	99.0	209.8	31.4
	2	50.7 ± 11.6	0.6	6500.0	26.6
	3	272.5 ± 104.9	0.4	284000.0	36.3
4	1	8.5 ± 3.6	99.8	148.8	41.7
	2	171.7 ± 62.5	0.2	110000.0	30.8
	3	0.0	0.0	0.0	0.0
5	1	9.2 ± 4.5	99.8	148.8	32.3
	2	43.8 ± 13.7	0.2	4610.0	42.4
	3	0.0	0.0	0.0	0.0
6	1	13.6 ± 1.6	99.3	295.8	14.5
	2	368.0 ± 43.0	0.6	565000.0	15.0
	3	0.0	0.0	0.0	0.0
7	1	14.3 ± 2.7	99.5	295.8	17.7
	2	288.8 ± 52.6	0.4	284000.0	19.4
	3	0.0	0.0	0.0	0.0
8	1	13.7 ± 3.7	96.7	295.8	21.6
	2	60.8 ± 15.2	1.3	9170.0	22.2
	3	1107.0 ± 236.4	2.0	6250000.0	20.6
9	1	8.7 ± 2.9	92.5	105.6	25.1
	2	28.2 ± 9.0	7.0	1650.0	28.5
	3	238.1 ± 109.3	0.5	202000.0	15.6
10	1	12.5 ± 3.4	99.5	295.8	23.8
	2	255.9 ± 42.0	0.5	51000.0	32.5
	3	0.0	0.0	0.0	0.0

Table 5C. Values of PdI, % of peak and mean size for 0.1 g L^{-1} LF at different pHs.

pH	Peak	Size (nm)	% Mass	kDa estimated	% Pd
		LF 0.1 g L^{-1} Electrolyte: 0.025M KCl			
3	1	11.9 ± 2.9	99.5	209.8	17.7
	2	224.2 ± 44.7	0.5	4610.0	19.9
	3	0.0	0.0	0.0	0.0
4	1	8.7 ± 3.6	99.9	74.9	24.5
	2	147.3 ± 32.3	0.1	101000.0	40.6
	3	0.0	0.0	0.0	0.0
5	1	11.5 ± 2.2	99.6	209.8	14.8
	2	242.7 ± 67.3	0.6	284000.0	12.9
	3	0.0	0.0	0.0	0.0
6	1	11.1 ± 2.9	98.7	209.8	22.5
	2	29.5 ± 7.1	0.9	2320.0	21.9
	3	255.6 ± 78.1	0.4	284000.0	14.3
7	1	13.0 ± 2.0	99.4	209.8	13.1
	2	122.9 ± 16.0	0.6	36400.0	13.7
	3	0.0	0.0	0.0	0.0
8	1	10.5 ± 2.0	97.9	148.8	34.1
	2	50.3 ± 14.4	1.6	4610.0	31.0
	3	434.5 ± 114.6	0.4	796000.0	21.0
9	1	8.2 ± 2.0	89.7	105.6	17.2
	2	18.9 ± 4.9	10.1	1710.0	21.7
	3	146.0 ± 38.1	0.2	101000.0	17.3
10	1	9.9 ± 4.2	99.8	105.6	31.7
	2	50.7 ± 18.0	0.1	6500.0	39.9
	3	157.0 ± 92.7	0.1	101000.0	49.9

Table 6C. Values of PdI, % of peak and mean size for 0.01 g L^{-1} LF at different pHs.

		LF 0.01g L^{-1} Electrolyte: 0.025M KCl			
pH	Peak	Size (nm)	%	kDa estimated	% Pd
3	1	13.7 ± 4.4	98.7	295.8	27.2
	2	250.8 ± 87.7	0.8	202000.0	23.9
	3	5262.3 ± 775.8	0.5	385000000.0	6.8
4	1	13.1 ± 2.6	99.4	295.8	19.6
	2	259.5 ± 49.1	0.6	284000.0	18.8
	3	0.0	0.0	0.0	0.0
5	1	11.7 ± 1.0	97.5	209.8	11.2
	2	580.1 ± 68.7	2.5	1120000.0	11.5
	3	0.0	0.0	0.0	0.0
6	1	13.0 ± 3.8	98.9	295.8	20.7
	2	220.8 ± 55.9	0.5	401000.0	25.2
	3	0.0	0.0	0.0	12.3
7	1	11.6 ± 2.1	95.7	209.8	17.7
	2	32. ± 6.6	1.0	2320.0	18.1
	3	825.0 ± 274.0	3.3	4430000.0	29.7
8	1	15.5 ± 3.9	98.3	417.0	20.6
	2	397.7 ± 62.6	1.7	284000.0	22.4
	3	0.0	0.0	0.0	0.0
9	1	12.0 ± 1.7	98.2	209.8	11.8
	2	365.9 ± 51.6	1.8	565000.0	12.0
	3	0.0	0.0	0.0	0.0
10	1	11.7 ± 2.2	95.3	209.8	18.0
	2	67.4 ± 13.2	1.5	18200.0	24.5
	3	941.9 ± 341.6	3.0	12400000.0	36.0

Highlights

➢ Accurate determination of the isoelectric points of BSA and LF under different separation conditions

➢ Accurate determination of the hydrodynamic size of BSA and LF under different separation conditions

➢ Determination of relevant surface properties for protein separation.